The Hydrophobic Region of the *Leishmania* Peroxin 14 – Requirements for Association with a Glycosome Mimetic Membrane

Normand Cyr[1,2§], Terry K Smith[3], Élodie Boisselier[4,5], Louis-Philippe Leroux[1,2], Anwer Hasil Kottarampatel[1,2], Amanda Davidsen[1,2], Christian Salesse[4,5], and Armando Jardim[1,2‡]

From the [1]Institute of Parasitology and [2]Centre for Host-Parasite Interactions, Macdonald Campus of McGill University, Ste-Anne-de-Bellevue QC, Canada, [3]Schools of Biology & Chemistry, Biomedical Sciences Research Complex, The North Haugh, The University, St. Andrews, Fife, Scotland, United Kingdom, [4]CUO-Recherche, Centre de recherche du CHU de Québec, Hôpital du Saint-Sacrement, Département d'ophtalmologie, Faculté de Médecine and [5]Regroupement stratégique PROTEO, Université Laval, Québec QC, Canada
.

Running Title: *Membrane insertion of LdPEX14*

Keywords: *Leishmania*, glycosome, PEX5, PEX14, protein targeting, membrane binding

‡To whom correspondence should be addressed: Institute of Parasitology, Macdonald Campus of McGill University, 21, 111 Lakeshore Road, Ste-Anne-de-Bellevue, Québec, Canada H9X 3V9. Phone: (514) 398-7727; Fax: (514) 398-7857, email: armando.jardim@mcgill.ca. Current address: [§]Department of Biochemistry and Molecular Medicine, Université de Montréal, Montréal QC, Canada.

Abbreviations - IPTG, isopropylthiogalactoside; PBS, phosphate buffered saline, PEX, peroxin; FBS, fetal bovine serum; LUV, large unilamellar vesicle.

Protein import into the *Leishmania* glycosome requires docking of the cargo loaded peroxin 5 (LdPEX5) receptor to the peroxin 14 (LdPEX14) bound to the glycosome surface. To examine the LdPEX14-membrane interaction, we purified *L. donovani* promastigote glycosomes and determined the phospholipid and fatty acid composition. These membranes contained predominately phosphatidylethanolamine, phosphatidylcholine, and phosphatidylglycerol modified primarily with C18 and C22 unsaturated fatty acid. Using large unilamellar vesicles (LUVs) with a lipid composition mimicking the glycosomal membrane in combination with sucrose density centrifugation and fluorescence activated cell sorting technique we established that the LdPEX14 membrane binding activity was dependent on a predicted transmembrane helix found within residues 149-179. Monolayer experiments showed that the incorporation of phosphatidylglycerol and phospholipids with unsaturated fatty acids, which increase membrane fluidity and favor a liquid expanded (LE) phase, facilitated the penetration of LdPEX14 into biological membranes. Moreover, we demonstrated that the binding of LdPEX5 receptor or LdPEX5-PTS1 receptor-cargo complex was contingent on the presence of LdPEX14 at the surface of LUVs.

Introduction

Proteins destined for the glycosome matrix typically contain one of two major topogenic sequences designated peroxisomal targeting signal 1 (PTS1) [1-3] or peroxisomal targeting signal 2 (PTS2) [4]. These signal sequences are bound by the *Leishmania* receptor proteins peroxin 5 (PEX5) and peroxin 7 (PEX7) which selectively bind the PTS1 and PTS2 motifs, respectively, with nanomolar affinities [5, 6]. RNAi experiments in the closely related parasite *Trypanosoma brucei* showed deletion or knockdown of either PEX5 or PEX7 levels caused mistargeting of PTS1 and PTS2 proteins, supporting the hypothesis that in kinetoplastid parasites both PEX5 and PEX7 are required for trafficking or translocation of cargo proteins into the glycosome [6-8].

A key component essential for the import of nascent polypeptides into glycosomes is LdPEX14. This protein is postulated to be part of a macromolecular complex proposed to form a convergence point to which the cargo loaded PEX5 and PEX7 receptors dock [9-14]. Although considerable advances have been made in identifying the machinery required for the trafficking and import of proteins into the glycosome, far less is known about the mechanisms that mediate association of proteins with the glycosome surface or translocation of large proteins across the glycosomal membrane. Accumulating evidence supports the notion that docking of cargo loaded PEX5 to the PEX14 containing importomer complex induces structural changes that promote the formation of a tightly gated channel or transient pore through which cargo proteins are postulated to pass [15-18].

Biophysical analysis showed that PEX14 in mammals, yeast (*Hansenula polymorpha*, *Pichia pastoris)* and trypanosomatids (*Trypanosoma brucei),* behaved as an integral membrane protein [7, 19-21]; whereas PEX14 from *Leishmania donovani* [22] and *Saccharomyces cerevisiae* [9] had characteristics typical of a peripheral membrane protein that is anchored to the

glycosome/peroxisome bilayer. Recent studies using recombinant *L. donovani* PEX14 (LdPEX14) illustrated that docking of *L. donovani* PEX5 (LdPEX5) induced conformational changes that involved a predicted transmembrane region spanning residues 149-179 of LdPEX14 [23], a domain that may be instrumental in the assembly of a translocation pore [15].

Here using biochemical and biophysical approaches we describe the phospholipid composition of the glycosomal membrane and demonstrate that the transmembrane domain on LdPEX14 is an important element mediating insertion of this protein into lipid bilayers that mimic the *L. donovani* glycosomal membrane. We show that membrane bound LdPEX14 is required for the association of LdPEX5 with LUVs but the LdPEX5-LdPEX14 interaction also promotes association of LdPEX5 with the lipid bilayer.

Materials and methods

Chemicals and reagents

Restriction endonucleases and DNA-modifying enzymes were purchased from Invitrogen or New England Biolabs. Horseradish peroxidase (HRP)-conjugated goat anti-rabbit IgG was purchased from GE Healthcare. HRP-conjugated goat anti-mouse was purchased from Sigma-Aldrich. Synthetic phospholipids and cholesterol (Chl) were obtained from Avanti Polar Lipids. All other reagents were of the highest quality commercially available.

Protein expression

The *L. donovani* PEX14 coding sequence and the internal deletion mutant lacking amino acids 149-179 (*ldpex14Δ149-179)* was generated by PCR based mutagenesis using the C-terminal hexahistidine-tagged pET30-*LdPEX14-His*$_6$. A fragment encompassing amino acids 120-200 of

LdPEX14 was amplified by PCR and cloned into the *Nde*I/*Xho*I sites of pET30b(+) to generate the pET30b-*ldpex14 (120-200)-His*$_6$ expression construct. LdPEX14/ldpex14 proteins were expressed in *E. coli* strain ER2566 and purified as previously described [23], except for ldpex14 (120-200) which was extracted from inclusion bodies prior to purification. LdPEX5 and ldpex5 truncated proteins and the *L. donovani* PTS1 protein hypoxanthine-guanine phosphoribosyltransferase (LdHGPRT) were purified as previously described [23-25]. Purified proteins were concentrated and the buffer exchanged for 40 mM Tris-HCl pH 8.0 150 mM NaCl (TBS150) using an Amicon Ultra filter unit (Millipore). The protein concentration was measured spectrophotometrically at 280 nm by the method of Pace *et al*. [26]. Purified proteins were stored at -80 °C.

Glycosome isolation

Leishmania donovani promastigotes (1.0 x 10^{12} cells) grown in DME-L media containing 10% FBS were harvested, washed twice with 10 ml of cold PBS, twice with 10 ml of hypotonic buffer (HB) (25 mM HEPES pH 7.2, 2 mM EGTA and 2 mM DTT), and incubated on ice for 20 min prior to lysis by expulsion through a 26 gauge needle until 95% lysis was achieved, as assessed by phase contrast microscopy. Lysates were made isotonic and cellular debris and nuclei were removed by centrifugation at 5,000 x *g* for 10 min at 4 °C. The supernatant was then centrifuged at 45,000 x *g* for 40 min to obtain a crude organelle pellet. The crude organelle pellet was re-suspended in 2.0 ml of 25 mM HEPES-NaOH, pH 7.4, applied to a 25-70% (w/v) sucrose gradient in 25 mM HEPES-NaOH pH 7.4, and then resolved by centrifugation at 125,000 x *g* for 16 h at 4 °C in a Beckman-Coulter SW28 rotor. The gradient was fractionated and the protein concentration of each fraction determined using the micro BCA assay (Thermo-Fisher). Fractions

were analyzed for acid phosphatase activity using 5 mM p-nitrophenol phosphate in 50 mM sodium acetate (lysosome and plasma membrane) and by Western blot using anti-LdPEX14 or anti-aldolase (glycosomal), anti-cytochrome oxidase IV (mitochondria), anti-Bip (endoplasmic reticulum), and anti-tubulin (plasma membrane and flagella). Fractions enriched for LdPEX14 were pooled, diluted four-fold with 25 mM HEPES, 150 mM NaCl and the organelle pellet collected by centrifugation at 45,000 x *g* for 1 h at 4 °C in a Beckman-Coulter Avanti JE centrifuge. The organelle pellet was re-suspended in 0.5 ml 25 mM HEPES, 150 mM NaCl and applied to a linear 20-40% Optiprep gradient in 25 mM HEPES 150 mM NaCl buffer and further resolved at 125,000 x *g* for 1 h at 4 °C on a Beckman-Coulter SW41 rotor. The gradient was fractionated (0.75 ml fractions) and analyzed using the above protocol. Fractions enriched for glycosomes were pooled and the purity evaluated by comparing the levels of LdPEX14 in 5 μg of cell lysates, the 45,000 *x* g pellet and supernatant and purified glycosomes.

Lipid composition of the glycosomal membrane

Phospholipids were extracted from purified glycosomes (300 μg total protein) using the Folch extraction protocol [27]. Phospholipids were separated by two-dimensional thin layer chromatography on Silica-G plates (EMD Chemicals) using the mobile phases chloroform:methanol:ammonia:water (90:74:12:8) in the first dimension and chloroform:methanol:acetone:acetic acid:water (40:15:15:12:8) in the second dimension. Phospholipids were visualized by charring plates sprayed with 2.0 M sulfuric acid and spots were quantified by phosphate analysis [28] and compared with a standard mixture containing, dioleylphosphatidylcholine (DOPC), dioleylphosphatidic acid (DOPA), dioleoyl-phosphatidylserine (DOPS), dioleoyl-phosphatidylethanolamine (DOPE), dioleoyl-

phosphatidylglycerol (DOPG), bovine brain sphingomyelin, and bovine phosphatidylinositol (PI). Phospholipid spots were scraped, digested with perchloric acid for 1 h at 150 °C and the inorganic phosphate quantified by the Bartlett method [29].

Mass spectrometry analysis of phospholipids

Phospholipid samples were suspended in chloroform/methanol (1:2 v/v) and analyzed by ESI-MS-MS on an ABSciex 4000 QTrap (linear ion trap). Samples were loaded into thin-wall nanoflow capillary tips and analysed with capillary voltages between 1.0-1.5 kV for both negative and positive ion modes, tandem mass spectra (MS-MS) was used with nitrogen as collision gas and various collision offset energies to obtain precursor and neutral loss scans both in positive and negative ion mode and MS-MS daughter ions scans were conducted to confirm identification.

Fatty acid composition of the glycosome phospholipids

Glycosome phospholipids dissolved in hexane containing the internal standard 1,2-diheptadecanoyl-*sn*-glycero-3-phosphoethanolamine (C17PE) (Avanti Polar Lipids) and sodium methoxide were incubated for 10 min at 20 ˚C [30]. Samples were extracted with hexane and 1 µl of the organic phase was injected onto a Varian CP-3800 gas chromatograph system equipped with a flame ionization detector, and a CP-Sil 88 capillary column (100 m x 0.25 mm, 0.20 µm film thickness, Varian). The injector and detector temperature were maintained at 260 °C and helium was used as the carrier gas while the oven temperatures was increased from 60 °C to 230 °C over a duration of 75 min. Methyl esters were identified by comparing retention times with a fatty acid methyl ester (FAME) standard mixture (Nu-Chek Prep, MN, USA). Quantification of the FAMEs

from C10 to C22:6 was calculated relative to the amount of the internal standard C17PE recovered using Galaxie software (Varian).

Liposome preparation

Individual phospholipids or mixtures of DOPE:DOPC:DOPG:PI:Chl (55:25:15:2.5:2.5; glycosome membrane mimetic mixture), DOPE:DOPC (2:1), DOPC:DOPG; (1:1), or DOPE:DOPG (1:1) were dissolved in chloroform and thin films were prepared by evaporation of the solvent under a nitrogen stream. Residual chloroform was removed under vacuum for 16 h. Multilamellar vesicles were prepared by re-suspending the lipid film in PBS at a concentration of 5 mg/ml. The suspension was then extruded through a 0.2 μm polycarbonate membrane (Millipore) to generate large unilamellar vesicles (LUV) with a diameter of 200 nm, a size comparable to *Leishmania* glycosomes [31].

Sucrose density flotation centrifugation

LUVs (500 μg) were incubated with proteins (20 μg of LdPEX14/ldpex14 variants or mixture of 20 μg of LdPEX14/ldpex14 variants and 15 μg of LdPEX5/ldpex5 variants) in 300 μl of PBS for 40 min at 25 °C, mixed with 1.2 ml of 66 % sucrose (w/v) in PBS, transferred to a 5.2 ml ultracentrifuge tube and overlaid with 3.0 ml of 40 % sucrose (w/v) in PBS, and then 1.0 ml of PBS. Samples were subjected to centrifugation at 75,000 x *g* for 16 h at 4 °C in a Beckman-Coulter SW55 rotor. The gradient was fractionated (0.65 ml/fraction) and the proteins were precipitated by the addition of sodium deoxycholate (0.2%), and trichloroacetic acid (15%). Protein pellets were acetone washed, resolved on SDS-PAGE sample buffer and proteins were visualized by

Western blot analysis using anti-LdPEX5 or anti-LdPEX14 rabbit antisera (1:5000) and goat anti-rabbit horseradish peroxidase-conjugated secondary antibody (1:10000; Sigma-Aldrich).

Alkaline carbonate extraction

LUVs loaded with LdPEX5, LdPEX14, or ldpex14 (120-200) were isolated by flotation and treated sequentially with 500 mM NaCl, 100 mM Na_2CO_3 pH 11.5, and 100 mM Na_2CO_3 pH 11.5 containing 4.0 M urea for 30 min at 0 °C [22]. Following each treatment samples were separated into a supernatant and pellet by centrifugation at 100,000 x *g* for 30 min at 4 °C in a TLA100.3 rotor on a Beckman-Coulter table top ultracentrifuge. Proteins in the pellet and supernatant fractions were precipitated with 15% TCA and then analyzed by Western blot.

Fluorescence Activated Cell Sorting (FACS) analysis

Recombinant LdPEX5 (5.0 mg/ml) was labelled with Oregon Green 514 succinimidyl ester dye and LdPEX14 (5.0 mg/ml) was labelled with Bodipy 630/650 succinimidyl ester dye (ThermoFisher Scientific) using the protocols outline by the manufacturer. Labelled proteins were purified by passing the reaction mixture (100 µl) through a 2.0 ml Sephadex G25 (0.8x4.0 cm) column and collecting the void volume fraction and protein concentrations measured spectrophotometrically [26]. The interaction of fluorescently tagged LdPEX5 and LdPEX14 with DOPE:DOPC:DOPG:PI:Chl LUVs was examined by pre-incubating alone or with 5 µg of LdPEX5, 5 µg of LdPEX14, or a mixture of 5 µg of LdPEX5 and 5 µg of LdPEX14 with 400 µg of LUVs in 400 µl of PBS for 15 min then diluting the sample to 2.0 ml with PBS for FACS analysis. Analyses were performed on a BD FACSAria calibrated with 300 nm beads (Sigma-Aldrich) and singlet LUV particles were gated on the basis of forward scatter height (FSC-H)

verses forward scatter area (FSC-A) on logarithmic scales. For LUV incubated with fluorescently tagged LdPEX5 and LdPEX14 the gates were determined to the LUV alone (negative control), and LUVs loaded with LdPEX14 exhibiting intermediate and high fluorescence intensities the gates were set arbitrarily based on the fluorescence of the two subpopulations.

Langmuir monolayer interactions

The binding of LdPEX14 to different phospholipid monolayers was performed on a Kibron DeltaPi-4 microtensiometer (Kibron Inc., Helsinki, Finland). The protein concentration required for surface saturation was determined using increasing protein concentration in the absence of phospholipids. Phospholipids were spread using a Hamilton syringe (Reno, NV, USA) at the surface of a trough containing 500 µl of 40 mM Tris HCl, 150 mM NaCl pH 7.8 buffer and the spreading solvent was allowed to evaporated until the surface pressure stabilized [32]. Measurements were performed with single phospholipid monolayers composed of DOPG, dimyristoyl phosphatidylglycerol (DMPG), palmitoyl-oleoyl phosphatidylglycerol (POPG) DOPE, DOPC, didocosahexaenoyl phosphatidylethanolamine (DDPE, 22:6) or a mixture of DOPE:DOPC:DOPG (55:25:20) or DOPE:DOPC:DOPG:DDPE (47:25:20:8). LdPEX14 was injected into the subphase of the monolayers at different initial surface pressures (Π_i) and the final surface pressure at equilibrium (Π_e) was monitored as a function of time. Plots of $\Delta\Pi$ ($\Delta\Pi = \Pi_e - \Pi_i$) as a function Π_i permitted the calculation of MIP (maximum insertion pressure) II_0 and synergy parameters [32, 33].

Limited proteolysis

Protein complexes in solution or bound to LUVs were re-suspended in 400 µl of PBS containing 1.0 mM $CaCl_2$ and 2.5 mM DTT then treated with clostripain (Worthington Biochemical Corp), at

a protease:substrate molar ratio of 1:50. The reaction was incubated at 0 °C and 75 µl aliquots were removed at 0, 2, 5 30, and 60 min time points. Digest mixtures were treated with 1.0 ml of ice-cold acetone to precipitated proteins for Western blot analysis. Bands on Western blot were quantified by densitometry and analyzed using NIH ImageJ software [34].

Bioinformatics

Hydropathicity analysis for LdPEX14 was performed using Kyte and Doolittle algorithm [35] and a three dimensional model of ldpex14 (120-200) was generated using the I-TASSER *ab initio* modeling server (zhanglab.ccmb.med.umich.edu/I-TASSER) [36]. The capacity of this fragment to form a helix was determined using the Jufo9D program [37]. Both TOPCONS [38] and TMHMM [39] programs were used to predict the transmembrane propensity of the helical fragment identified by Jufo9D.

Results

Glycosome purification and phospholipid composition

Using subcellular fractionation *L. donovani* promastigote glycosomes were ~20-fold enriched using a sucrose and Optiprep density gradient as previously described [6]. Crude glycosomes fractionated on a linear sucrose density gradient and screened for acid phosphatase activity showed that the fragments of plasma membrane or lysosome partitioned with fractions 2-10 (Fig. 1A). Western blot analysis using anti-LdPEX14, confirmed that glycosomes were predominantly recovered in fractions 20-25 near the bottom of the gradient (Fig. 1B). Similar analyses with anti-cytochrome oxidase IV (COX IV) antibodies showed that mitochondria were predominantly

recovered in the 5,000 x *g* fraction. Analysis of the sucrose gradient fractions with the anti-COX IV and anti-tubulin antibodies showed minimal mitochondrial, plasma membrane, or flagella contamination of the glycosomes in fractions 20-25. Western blot analysis of pooled glycosomes collected from the Optiprep gradient using anti-LdPEX14 showed that glycosomes were ~20- and 4-fold enriched when compared to whole cell lysate or the 45, 000 x *g* pellet, respectively (Fig. 1C).

Analysis of the *L. donovani* glycosomal membrane phospholipid composition by 2D-TLC showed four major spots with a relative abundance of 52 ± 5%, 22 ± 4%, 16 ± 5%, 6 ± 2%, and 3 ± 1% based on phosphate determination (Table I, Fig 2A), which were identified as phosphatidylcholine (PC), phosphatidylethanolamine (PE), phosphatidylglycerol (PG), and phosphatidylinositol (PI) and inositol-phosphocermide (IPC) using the phospholipid standard mixture containing DOPC, DOPE, DOPS, DOPA, DOPG, phosphoinositol and sphingomyelin. This revealed that the *Leishmania* glycosomal membrane had an ~8-fold higher phosphatidylglycerol content (Table I) when compared to the plasma membrane composition (16% vs 2%) [40].

Electrospray mass spectrometry (ESI-MS/MS) analysis of the glycosome phospholipids using both positive and negative ion modes confirmed the presence of five major classes of phospholipids: phosphatidylethanolamine (PE), phosphatidylcholine (PC), phosphatidylglycerol (PG), phosphatidylinositol (PI) and inositol-phosphoceramide (IPC) (Fig. 2B & 2C). Mass spectrometry analysis also detected the presence of sphingolipid ceramide that was not resolved as with the solvent systems used for the 2D-TLC analysis as this lipid is predicted to migrate with the solvent front.

Fatty acid analysis by gas chromatography revealed that ~60% of the fatty acid content of the glycosomal membrane phospholipids was 18-carbon long fatty acid chains (C18), with the unsaturated fatty acids C18:1 and C18:2 being the most abundant (Table II). In addition, the *L. donovani* glycosomal membrane contained significant amounts of the longer chain C22:5 fatty acid (~15% of total fatty acids). Interestingly, ~47% of the fatty acid content of these phospholipids was polyunsaturated (Table II), a feature that contributes to an increased membrane fluidity [41].

LdPEX14-membrane interaction

Sucrose density flotation experiments were performed using LUVs mimicking the *L. donovani* glycosomal membrane phospholipid composition to evaluate the LdPEX14-membrane interaction. Incubation of LdPEX14 with DOPE:DOPC:DOPG:PI:Chl LUVs showed that a significant portion of the recombinant protein bound to these model membranes floated to the top of the sucrose gradient (Fig. 3A). In the absence of LUVs, no LdPEX14 flotation was observed. Addition of 500 mM NaCl, a salt concentration typically used to disrupt electrostatic interactions with the membrane surface, did not alter the binding of LdPEX14 to LUVs. This suggested that the LdPEX14-membrane association was stabilized by hydrophobic contacts with the lipid bilayer core (Table I, Fig. 3A). Interestingly, incubating LdPEX14 with LUVs at 0 °C or 23 °C prior to flotation revealed that ~50-70% of LdPEX14 was recruited to the LUV membranes; whereas at 37 °C, near quantitative binding of LdPEX14 to LUVs was obtained (Fig. 3B).

LUVs loaded with LdPEX14 and purified by sucrose flotation were sequentially extracted with 500 mM NaCl and 100 mM alkaline carbonate, treatments used to evaluate the membrane-protein interaction. In both cases LdPEX14 partitioned with the LUV membrane pellet, a biophysical behaviour diagnostic of a protein forming contacts with the hydrophobic core the lipid bilayer (Fig.

3C). A more stringent extraction of the LUV membrane pellet with 100 mM alkaline carbonate containing 4.0 M urea resulted in an equal distribution of LdPEX14 between the supernatant and membrane pellet fraction (Fig. 3C), further supporting the conjecture that this interaction was stabilized by nonpolar contacts [42].

To examine if membrane association altered the LdPEX14 structure, a limited proteolytic analysis was performed using the arginine specific endoproteinase clostripain. In the absence of LUVs LdPEX14 exhibited a high susceptibility to proteolytic cleavage and was complete degraded within 5 min (Fig. 3D). In contrast, membrane bound LdPEX14 exhibited a marked resistance to proteolysis and resulted in ~50 % of the full length LdPEX14 remaining after a 30 min incubation and is suggestive of a membrane insertion which triggers structural changes that render LdPEX14 more resistant to proteolysis (Fig. 3D). It should be noted that some degradation of LdPEX14 was detected in these Western blots. This is attributed to the extreme susceptibility of this protein to proteolysis arising from its predicted native disordered structure (unpublished data).

The hydrophobic region of LdPEX14 is required for membrane attachment

A hydropathicity analysis of the LdPEX14 protein revealed that a region spanning residues 120-200 (Fig. 4A & 4B) contained a putative transmembrane helix (residues 154-174) (Fig. 4A, *solid line*) circumscribed by a proline rich random coil region (residues 120-152) corresponding to the *Leishmania* PEX7 binding site [6], and an arginine rich region (residues 182-200, *highlighted in red*) located downstream of the putative transmembrane helix, a structure known to have membrane binding activity [43]. *Ab initio* modeling of residues 154-174 using the I-TASSER algorithm indicated that this region favors a helical structure spanning 15 amino acids and measuring 22.4 Å in length (α-carbon to α-carbon) (Fig. 4C).

Additionally, intrinsic fluorescence measurements using W152 from ldpex14(120-200) as an environmental probe showed a strong hypsochromic shift in the maximum wavelength of fluorescence emission of W152 indicating that this region inserts into the hydrophobic environment of the lipid bilayer (Fig. S1A). Likewise, acrylamide quenching experiments revealed higher quenching constants (dynamic component: 9.6 M-1, static component: 0.8 M-1) in the absence of liposomes whereas a Stern-Volmer constant of 3.0 M-1 was observed in the presence of liposomes (Fig. S1B and S1C), indicating that W152 was more accessible to quenching in the absence of liposomes.

To verify that this hydrophobic region was required for membrane association, an internal deletion mutant lacking residues 149-179 (ldpex14Δ149-179) was generated and membrane binding assessed by sucrose density flotation. Unlike the full length LdPEX14, which exhibited robust binding to DOPE:DOPC:DOPG:PI:Chl LUVs (Fig. 5A), no interaction of ldpex14Δ149-179 with LUVs was detected. This observation supports the notion that residues 149-179 formed a structural element required for membrane association (Fig. 5A). To validate this hypothesis a recombinant protein fragment encompassing residues 120-200 (ldpex14 (120-200)) generated and assayed for membrane binding activity. The ldpex14 (120-200) fragment was found to quantitatively bind the glycosome mimetic LUVs (Fig. 5A).

Anionic phospholipids are required for LdPEX14 membrane binding

The role of the phospholipid composition of lipid bilayers in mediating the LdPEX14-membrane interaction was examined using liposomes composed of the single phospholipids DOPC, DOPG, or DOPS or a mixture of DOPE:DOPC, DOPC:DOPG, and DOPE:DOPG or hexagonal phase II structures composed of DOPE or DOPA. Sucrose density flotation experiments showed a robust

binding and flotation of LdPEX14 associated with DOPA, DOPG, DOPS, DOPC:DOPG (1:1) and DOPE:DOPG (1:1) vesicles (Fig. 5B). However, no significant binding was detected with DOPC, DOPE, or DOPE:DOPC (2:1) phospholipid (Fig. 5C) which suggested that anionic phospholipids were required for LdPEX14 association with lipid bilayers.

Fluorescence activated cell sorting (FACS) was used as a second independent method to corroborate the LdPEX14-LUV interaction. For this technique, LdPEX5 and LdPEX14 were labelled with the fluorescent dyes Oregon Green and Bodipy 630/650, respectively, then mixed with LUVs and analyzed by flow cytometry. PEX-free LUVs displayed low autofluorescence in both channel used (Fig. 6A), as expected. Oregon Green-labelled LdPEX5 alone failed to bind to LUVs, as determined by the arguably small increase in fluorescence detected on the LUVs (Fig. 6B). In stark contrast, LUVs incubated with LdPEX14 tagged with Bodipy 630/650 fluorescent dye segregated two LUV populations with intermediate (~58% of LUVs) and high fluorescence intensities (~16%). The variation in the fluorescence intensities likely corresponds to difference in the number of LdPEX14 molecules bound to per LUV (Fig. 6C). Addition of Oregon Green tagged-LdPEX5 to LUVs loaded with LdPEX14 resulted into additional subpopulations of LUVs with intermediate (~22%) and high fluorescence intensities (~9%) that contain both LdPEX5 and LdPEX14 (Fig. 6D). These results also confirm that the association of LdPEX5 with the LUVs is dependent LdPEX14.

Insertion of LdPEX14 into phospholipid monolayers

To investigate the effect of the phospholipid head groups and lipid packing on LdPEX14 insertion into membranes, experiments were performed using monolayers of defined phospholipid composition as previously described [32, 33, 44]. Prior to these experiments, the surface binding

activity of LdPEX14 or ldpex14Δ149-179 was assessed by monitoring the increase in surface pressure at the air-buffer interface as a function of protein concentration [44]. As shown in Figure 7A, saturation of the air-buffer interface was observed when 0.31 μM of LdPEX14 was added to the subphase, which resulted in a maximum pressure of 23.9 mN/m. In contrast, saturation of the air-buffer surface with ldpex14Δ149-179 was observed using a protein concentration of ~0.86 μM at a lower pressure of 21.2 mN/m (Fig. 7A). In addition, the kinetics of LdPEX14 binding is much faster than that of LdPEX14-Δ49-179 (Fig. 7B). Altogether, these data suggest that LdPEX14 has a much larger surface activity than LdPEX14-Δ149-179, thus highlighting the importance of the transmembrane segment of LdPEX14 in its membrane binding. The additional measurements were thus solely performed using LdPEX14. The impact of phospholipid head groups on LdPEX14 membrane interaction was examined using monolayers with increasing lateral initial surface pressure (Π_i), which reflects the degree of lipid packing [32, 33, 44, 45], and the change in surface pressure ($\Delta\Pi$) was monitored following injection of 0.31 μM LdPEX14 into the subphase. Linear regression plots of $\Delta\Pi$ versus Π_i permitted determination of the maximum insertion pressure (MIP) at which LdPEX14 would penetrate into lipid monolayer and the synergy factor (Fig. 7C) which provides a measure of the affinity of LdPEX14 for the lipid monolayer [32, 33].

Monolayers composed of DOPG, DOPC, and DOPE, lipids with a similar phase transition temperature of -16 to -18 °C [46], showed that DOPG monolayers exhibited the highest MIP following LdPEX14 insertion into the monolayers (Fig. 8A). The synergy factor, an indicator of the favourability of the interaction between a protein and phospholipid monolayer (Fig. 8B), also confirmed that the DOPG monolayer had greatest affinity for LdPEX14, an observation supported by LUV binding using sucrose density flotation experiments (Fig. 5B). Similarly, the rate of absorption was higher for DOPG (Fig. S2). In addition, the lowest values of MIP and synergy have

been obtained with DOPE, which is also consistent with the measurements performed using LUVs (Fig. 5B).

To study the interaction of LdPEX14 with membranes that mimic the composition of the glycosomal membrane, mixed monolayers containing DOPE:DOPC:DOPG (55:25:20) were used. Surprisingly, the values of MIP and synergy parameters for mixed monolayers were significantly smaller than those obtained with monolayers containing only DOPG (Fig. 8A & 8B). However, an interesting feature of the glycosomal membrane was the high proportion of unsaturated long chain C22 fatty acids (Table I). Incorporating the phospholipid DDPE containing the long chain C22:6 fatty acid into mixed monolayers with composition DOPE:DOPC:DOPG:DDPE (47:25:20:8) showed enhanced LdPEX14 binding as reflected by the increase in the MIP and synergy values (Fig. 8A & 8B); albeit the value of synergy is lower values then observed with DOPG monolayers.

The latter experiment suggested that the degree of fatty acid unsaturation and monolayer fluidity both influenced LdPEX14 binding. To test this hypothesis monolayers composed of DMPG, POPG, or DOPG; phospholipids with liquid crystalline to solid crystalline gel phase transition temperature of 23 °C, -1 °C, and -18 °C, respectively [46], were prepared and LdPEX14 insertion was monitored. Monolayer composed of DMPG and POPG, which at 20 °C have reduced fluidity, exhibited lower MIP and synergy values when compared to DOPG monolayers (Fig. 8C & 8D). These data indicate that lipid packing has an impact on LdPEX14 insertion into membranes and an increased fluidity favors the insertion of LdPEX14.

LdPEX14 is required for LdPEX5 association with LUVs

LdPEX14 is proposed to function as a docking complex that facilitates the binding of cargo loaded LdPEX5 receptor to the glycosome surface. To validate this model, glycosome mimetic LUVs

alone or loaded with LdPEX14 were used. Addition of LdPEX5 or the LdPEX5-PTS1 complex to DOPE:DOPC:DOPG:PI:Chl LUVs showed that this receptor alone or loaded with the PTS1 cargo protein LdHGPRT (PTS1) [47] showed not binding to LUVs (Fig. 9A & 9B). Similarly, no binding was detected when LdHGPRT (PTS1) alone was added to LUVs loaded with LdPEX14 (Fig. 9C). However, addition of LdPEX5 or LdPEX5-PTS1 to LUVs charged with LdPEX14 resulted in robust binding of LdPEX5 and LdHGPRT to LUVs (Fig. 9D & 9E). These data confirm that the recruitment of LdPEX5 is dependent on its association with membrane bound LdPEX14 since no LdPEX5 binding was detected with LUVs loaded ldpex14 (Δ149-179) (Fig. 9F), a variant LdPEX14 that is known to bind LdPEX5 in solution [23], but not LUVs mimicking the glycosomal membrane (Fig. 5A).

Previous studies reveal that in solution LdPEX5-LdPEX14 interaction was depend on the W_{293} AQEY_{297} motif on LdPEX5 [48, 49]. To evaluate if this motif was required for the association of LdPEX5 with LUV bound LdPEX14, sucrose density flotation experiment were performed by mixing LdPEX5 or ldpex5 N-terminal truncation constructs with LUVs in the presence and absence of LdPEX14. It should be noted that none of the ldpex5 N-terminal truncation constructs lacking the first 205 residues (ldpex5 (205-625)), 268 residues (ldpex5 (268-625)) or 303 residue (ldpex5 (303-625)) or the internal ldpex5 fragment spanning residues 203-391 (ldpex5 (203-391)) alone bound to the DOPE:DOPC:DOPG:PI:Chl LUVs. Western blot analysis demonstrated that the latter ldpex5 proteins were all detected at the bottom of the sucrose density gradient (Fig. 10A). However, in the presence of LdPEX14 bound to LUVs, ldpex5 (205-652), ldpex5 (268-625) and the internal fragment ldpex5 (203-391) all floated and were at the top of the sucrose gradient (Fig. 10A, *right panel*). In contrast, no flotation of the N-terminal truncation variant ldpex5 (303-625)

was observed. This is likely due the absence of the region required for the interaction with LdPEX14.

To examine the association of the LdPEX5-LdPEX14 complex with membranes, LdPEX14 or LdPEX5-LdPEX14 loaded LUVs purified by sucrose density flotation centrifugation were sequentially extracted with NaCl, alkaline carbonate, and alkaline carbonate/urea (Fig. 3C). However, similar extractions of LUVs loaded with LdPEX5-LdPEX14 revealed that >90% of the LdPEX14 was retained in the membrane pellet (Fig. 10B). The data suggest that the binding of LdPEX5 alters the interaction of LdPEX14 with the lipid bilayer which increases the hydrophobic contacts with the membrane. More surprisingly was the observation that LdPEX5, a soluble protein without a predicted transmembrane domain, remained highly refractory to alkaline carbonate/urea extraction. It is likely that the LdPEX5-LdPEX14 interaction is extremely stable and resistant to alkaline carbonate/urea treatment [48, 49]. In contrast to LdPEX5, which requires LdPEX14 for membrane interaction, the mammalian and yeast PEX5 alone were sufficient for membrane insertion [15, 17, 50].

Discussion

PEX14 is a vital biogenesis component required for the docking/translocation machinery that participates in formation of a dynamic pore that mediates the import of folded proteins or protein complexes across the glycosome/peroxisome membrane [7, 9, 12, 13, 15, 51-53]. Native LdPEX14 isolated from glycosomes is part of an ~800 kDa complex that is anchored as a peripheral membrane protein to the cytosolic face of the glycosomal membrane [23, 54]. Lipidomic analysis of the *L. donovani* glycosome revealed that this organellar membrane contained elevated levels of phosphatidylethanolamine and phosphatidylglycerol (Table I); phospholipids with a small head group that would impart a lower lateral membrane pressure and confer an anionic charge on these membranes [55]. Moreover, fatty acid analysis showed that that phospholipids of the glycosomal membrane, and in particular phosphatidylglycerol, were preferentially modified with polyunsaturated C18 and C22 fatty acids; fatty acids that are enriched in *Leishmania* [56]. Collectively, the physiochemical properties of the phospholipids of glycosome membrane are predicted to increase the membrane fluidity which would facilitate mobility and structural rearrangement of proteins in the bilayer [57, 58]; features that may be critical for LdPEX14 insertion, oligomerization, and transient pore formation on the glycosomal membrane [59]. This conjecture is further supported by experiments in this study showing that incorporation of DOPG (C18:1) and DDPE (C22:6) into monolayer favored an increase in the maximum insertion pressure and synergy factor [33] associated with the insertion of LdPEX14. In contrast, the mammalian, yeast, and *T. brucei* peroxisomal/glycosomal membranes have lipid compositions enriched in phosphatidylcholine and the negatively charged lipid phosphatidylinositol [60-62], which may influence the interaction of the PEX14 homologues with these membranes.

Binding studies performed using sucrose density flotation or FACS techniques both corroborated the hypothesis that recombinant LdPEX14 can spontaneously insert into model membranes that mimic the composition of the *Leishmania* glycosome. This association was critically dependent on residues 149-179, a segment calculated to adopt a hydrophobic transmembrane α-helix. Smaller fragments of ldpex14 that encompass residues 120-200 also spontaneously bound to LUVs.

Monolayer experiments confirmed that the phospholipid head groups had a profound influence on membrane insertion, with DOPG dramatically favoring LdPEX14 penetration into biological membranes as reflected by the MIP and synergy parameters. Incorporating even modest levels of DOPG, ~20 mole percent, into mixed membranes, levels comparable to those detected in the glycosomal membrane was sufficient to promote LdPEX14 insertion. In contrast, monolayer composed of DOPE or DOPC exhibited a diminished LdPEX14 insertion activity which suggests that negatively charged lipids are important for recruiting LdPEX14 to biological membrane. This contention is further supported by the observation that high salt concentrations caused a marked decrease in the synergy values. The synergy values of ~0.35 suggest that LdPEX14 insertion is favored with lipid bilayers in a liquid crystalline state [45] such as the glycosomal membrane which contains a high content of unsaturated fatty acids. Increased membrane fluidity is likely to be critical for the dynamic recruitment, insertion, and structural rearrangements of proteins associated with the formation of the transient translocation pore on the glycosomal membrane.

A key event in the import of proteins into the glycosome matrix involves the formation of a transient pore following the docking of the LdPEX5 receptor loaded with a PTS1 cargo to the glycosome-associated LdPEX14 [15, 63]. Here we demonstrated using sucrose density flotation and FACS experiments that the binding of LdPEX5, to LUVs was critically dependent on the

presence of LdPEX14 bound to the vesicle membrane. Interestingly, extraction of LUVs loaded with the LdPEX5-LdPEX14 complex, using stringent conditions that included both alkaline carbonate and 4 M urea suggested that following recruitment LdPEX5 inserted into the lipid bilayer where it is postulated to participate in the formation of a transient pore [16, 64]. However, since LdPEX5 does not contain any predicted transmembrane domains it is likely that this protein does not form direct contacts with the lipid bilayer but remains tightly associated with the membrane bound LdPEX14 [48, 49, 65]. Truncation mapping studies confirmed that the binding of LdPEX5 with LUV bound LdPEX14 was depend on residues 268-303, a region containing a WAQEY motif that binds LdPEX14 with a low nanomolar affinity [48]. Finally, the studies provide a framework required to dissect the protein-membrane interactions and the molecular events associated with the binding of PTS1 and PTS2 loaded receptors to the LdPEX14 containing complex and subsequent transient pore formation on the glycosome mimetic membranes.

Abbreviations

IPTG, isopropylthiogalactoside; PBS, phosphate buffered saline, PEX, peroxin; FBS, fetal bovine serum; LUV, large unilamellar vesicle.

Author contribution

N.C. and A.J. conceived, designed experiments and wrote the manuscript. T.K.S. contributed to the analysis and phospholipid identification. L.P.L. generated data in figure 6 and edited the manuscript. E.B., C.S. and N.C. designed and contributed to the analysis of phospholipid monolayer experiments and assisted with editing the manuscript. A.H.K. and A.D contributed data to figures 9 and 10.

Funding

This work was funded by operating grants from the Canadian Institutes of Health Research (CIHR) and a Fonds de recherche du Québec – Nature et technologies (FRQNT) Regroupement Stratégique grant to the Centre for Host-Parasite Interactions (AJ). NC was supported by a doctoral research scholarships from FRQNT. EB was supported by a Banting postdoctoral fellowship from CIHR. This work was also supported in part by Wellcome Trust grants 086658 and 093228 to TKS. CS recognizes the financial support from the Natural Sciences and Engineering Research Council of Canada and a Canada Foundation for Innovation grant 16299.

Acknowledgements

The authors acknowledge the technical help of Dr. H. A. Weiler and Mr. J. Deguire (McGill U.) for providing access to the gas chromatograph for the analysis of glycosomal membrane fatty acids and M. Niemann and A. Schneider (U. Bern) and J. Bangs (SUNY) for generously providing the anti-cytochrome oxidase IV and anti-Bip antibodies respectively.

Competing Interests

Authors have no competing interests asssociated with the manuscript.

References

1 Blattner, J., Swinkels, B., Dorsam, H., Prospero, T., Subramani, S. and Clayton, C. (1992) Glycosome assembly in trypanosomes: variations in the acceptable degeneracy of a COOH-terminal microbody targeting signal. J. Cell. Biol. **119**, 1129-1136

2 Keller, G. A., Krisans, S., Gould, S. J., Sommer, J. M., Wang, C. C., Schliebs, W., Kunau, W., Brody, S. and Subramani, S. (1991) Evolutionary conservation of a microbody targeting signal that targets proteins to peroxisomes, glyoxysomes, and glycosomes. J. Cell Biol. **114**, 893-904

3 Gould, S. J., Keller, G. A. and Subramani, S. (1988) Identification of peroxisomal targeting signals located at the carboxy terminus of four peroxisomal proteins. J. Cell Biol. **107**, 897-905

4 Swinkels, B. W., Gould, S. J., Bodnar, A. G., Rachubinski, R. A. and Subramani, S. (1991) A novel, cleavable peroxisomal targeting signal at the amino-terminus of the rat 3-ketoacyl-CoA thiolase. EMBO J. **10**, 3255-3262

5 Jardim, A., Liu, W., Zheleznova, E. and Ullman, B. (2000) Peroxisomal targeting signal-1 receptor protein PEX5 from *Leishmania donovani* : Molecular, biochemical, and immunocytochemical characterization. J. Biol. Chem. **275**, 13637-13644

6 Pilar, A. V., Madrid, K. P. and Jardim, A. (2008) Interaction of *Leishmania* PTS2 receptor peroxin 7 with the glycosomal protein import machinery. Mol. Biochem. Parasitol. **158**, 72-81

7 Furuya, T., Kessler, P., Jardim, A., Schnaufer, A., Crudder, C. and Parsons, M. (2002) Glucose is toxic to glycosome-deficient trypanosomes. Proc. Natl Acad. Sci. USA. **99**, 14177-14182

8 Galland, N., Demeure, F., Hannaert, V., Verplaetse, E., Vertommen, D., Smissen, P. V. D., Courtoy, P. J. and Michels, P. A. M. (2007) Characterization of the role of the receptors PEX5 and PEX7 in the import of proteins into glycosomes of *Trypanosoma brucei*. Biochim. Biophys. Acta. **1773**, 521-535

9 Albertini, M., Rehling, P., Erdmann, R., Girzalsky, W., Kiel, J. A., Veenhuis, M. and Kunau, W. H. (1997) Pex14p, a peroxisomal membrane protein binding both receptors of the two PTS-dependent import pathways. Cell. **89**, 83-92

10 Fransen, M., Terlecky, S. R. and Subramani, S. (1998) Identification of a human PTS1 receptor docking protein directly required for peroxisomal protein import. Proc. Natl. Acad. Sci. **95**, 8087-8092

11 Bottger, G., Barnett, P., Klein, A. T. J., Kragt, A., Tabak, H. F. and Distel, B. (2000) *Saccharomyces* cerevisiae PTS1 receptor Pex5p interacts with the SH3 domain of the peroxisomal membrane protein Pex13p in an unconventional, non-PXXP-related manner. Mol. Biol. Cell. **11**, 3963-3976

12 Miyata, N. and Fujiki, Y. (2005) Shuttling Mechanism of Peroxisome Targeting Signal Type 1 Receptor Pex5: ATP-Independent Import and ATP-Dependent Export. Mol. Cell. Biol. **25**, 10822-10832

13 Otera, H., Setoguchi, K., Hamasaki, M., Kumashiro, T., Shimizu, N. and Fujiki, Y. (2002) Peroxisomal Targeting Signal Receptor Pex5p Interacts with Cargoes and Import Machinery Components in a Spatiotemporally Differentiated Manner: Conserved Pex5p WXXXF/Y Motifs Are Critical for Matrix Protein Import. Mol. Cell Biol. **22**, 1639-1655

14 Otera, H., Harano, T., Honsho, M., Ghaedi, K., Mukai, S., Tanaka, A., Kawai, A., Shimizu,

N. and Fujiki, Y. (2000) The mammalian peroxin Pex5pL, the longer isoform of the mobile Peroxisome Targeting Signal (PTS) type 1 transporter, translocates the Pex7p-PTS2 protein complex into peroxisomes via its initial docking site, Pex14p. J. Biol. Chem. **275**, 21703-21714

15 Meinecke, M., Cizmowski, C., Schliebs, W., Kruger, V., Beck, S., Wagner, R. and Erdmann, R. (2010) The peroxisomal importomer constitutes a large and highly dynamic pore. Nat. Cell Biol. **12**, 273-277

16 Erdmann, R. and Schliebs, W. (2005) Peroxisomal matrix protein import: the transient pore model. Nat. Rev. Mol. Cell Biol. **6**, 738-742

17 Kerssen, D., Hambruch, E., Klaas, W., Platta, H. W., de Kruijff, B., Erdmann, R., Kunau, W. H. and Schliebs, W. (2006) Membrane association of the cycling peroxisome import receptor Pex5p. J. Biol. Chem. **281**, 27003-27015

18 Gouveia, A. M., Guimaraes, C. P., Oliveira, M. E., Reguenga, C., Sa-Miranda, C. and Azevedo, J. E. (2003) Characterization of the Peroxisomal Cycling Receptor, Pex5p, Using a Cell-free in Vitro Import System. J. Biol. Chem. **278**, 226-232

19 Komori, M., Rasmussen, S. W., Kiel, J. A., Baerends, R. J., Cregg, J. M., van der Klei, I. J. and Veenhuis, M. (1997) The *Hansenula polymorpha* PEX14 gene encodes a novel peroxisomal membrane protein essential for peroxisome biogenesis. EMBO J. **16**, 44-53

20 Shimizu, N., Itoh, R., Hirono, Y., Otera, H., Ghaedi, K., Tateishi, K., Tamura, S., Okumoto, K., Harano, T., Mukai, S. and Fujiki, Y. (1999) The peroxin Pex14p. cDNA cloning by functional complementation on a Chinese hamster ovary cell mutant, characterization, and functional analysis. J. Biol. Chem. **274**, 12593-12604

21 Will, G. K., Soukupova, M., Hong, X., Erdmann, K. S., Kiel, J. A. K. W., Dodt, G., Kunau, W.-H. and Erdmann, R. (1999) Identification and Characterization of the Human Orthologue of Yeast Pex14p. Mol. Cell Biol. **19**, 2265-2277

22 Jardim, A., Rager, N., Liu, W. and Ullman, B. (2002) Peroxisomal targeting protein 14 (PEX14) from *Leishmania donovani*. Molecular, biochemical, and immunocytochemical characterization. Mol. Biochem. Parasitol. **124**, 51-62

23 Cyr, N., Madrid, K. P., Strasser, R., Aurousseau, M., Finn, R., Ausio, J. and Jardim, A. (2008) *Leishmania donovani* Peroxin 14 undergoes a marked conformational change following association with Peroxin 5. J. Biol. Chem. **283**, 31488-31499

24 Allen, T., Hwang, H.-Y., Wilson, K., Hanson, S., Jardim, A. and Ullman, B. (1995) Cloning and expression of the adenine phosphoribosyltransferase gene from *Leishmania donovani*. Mol. Biochem. Parasitol. **74**, 99-103

25 Madrid, K. P., De Crescenzo, G., Wang, S. and Jardim, A. (2004) Modulation of the *Leishmania donovani* peroxin 5 quaternary structure by peroxisomal targeting signal 1 ligands. Mol. Cell. Biol. **24**, 7331-7344

26 Pace, C. N., Vajdos, F., Fee, L., Grimsley, G. and Gray, T. (1995) How to measure and predict the molar absorption coefficient of a protein. Protein Sci. **4**, 2411-2423

27 Folch, J., Lees, M. and Stanley, G. H. (1957) A simple method for the isolation and purification of total lipides from animal tissues. J Biol Chem. **226**, 497-509

28 Feng, J., Chen, Y., Pu, J., Yang, X., Zhang, C., Zhu, S., Zhao, Y., Yuan, Y., Yuan, H. and Liao, F. (2011) An improved malachite green assay of phosphate: Mechanism and application. Ana. Biochem. **409**, 144-149

29 Bartlett, S. G. (1959) Phosphorus assay in column chromatography. J. Biol. Chem. **234**, 466-468

30 Marinetti, G. V. (1962) Hydrolysis of lecithin with sodium methoxide. Biochemistry **1**, 350-353
31 Hart, D. T. and Opperdoes, F. R. (1984) The occurence of glycosomes (microbodies) in the promastigote stage of four major *Leishmania* species. Mol. Biochem. Parasitol. **13** 159-172
32 Calvez, P., Bussières, S., Éric, D. and Salesse, C. (2009) Parameters modulating the maximum insertion pressure of proteins and peptides in lipid monolayers. Biochemie. **91**, 718-733
33 Boisselier, E., Calvez, P., Demers, E., Cantin, L. and Salesse, C. (2011) Influence of the physical state of phospholipid monolayers on protein binding. Langmuir **28**, 9680-9688
34 Abramoff, M. D., Magelhaes, P.J., Ram, S.J.. (2004) Image processing with ImageJ. Biophotonics Intl. **11**, 36-42
35 Kyte, J. and Doolittle, R. F. (1982) A simple method for displaying the hydropathic character of a protein. J. Mol. Biol. **157**, 105-132
36 Zhang, Y. (2008) I-TASSER server for protein 3D structure prediction. BMC Bioinformatics. **9**, 40
37 Leman, J. K., Mueller, R., Karakas, M., Woetzel, N. and Meiler, J. (2013) Simultaneous prediction of protein secondary structure and transmembrane spans. Proteins: Struct., Funct., Bioinf. **81**, 1127-1140
38 Tsirigos, K. D., Peters, C., Shu, N., Käll, L. and Elofsson, A. (2015) The TOPCONS web server for consensus prediction of membrane protein topology and signal peptides. Nuc Acids Res. **43**, W401-W407
39 Krogh, A., Larsson, B., von Heijne, G. and Sonnhammer, E. L. L. (2001) Predicting transmembrane protein topology with a hidden markov model: application to complete genomes, edited F. Cohen. J. Mol. Biol. **305**, 567-580
40 Rakotomanga, M., Blanc, S., Gaudin, K., Chaminade, P. and Loiseau, P. M. (2007) Miltefosine affects lipid metabolism in *Leishmania donovani* promastigotes. Antimicrob. Agents Chemother. **51**, 1425-1430
41 Sánchez-Martín, M. J., Ramon, E., Torrent-Burgués, J. and Garriga, P. (2008) Improved conformational stability of the visual G Protein-Coupled Receptor Rhodopsin by specific interaction with docosahexaenoic acid phospholipid. ChemBioChem. **14**, 639-644
42 Brass, V., Bieck, E., Montserret, R., Wolk, B., Hellings, J. A., Blum, H. E., Penin, F. and Moradpour, D. (2002) An amino-terminal amphipathic α-helix mediates membrane association of the Hepatitis C virus nonstructural protein 5A. J. Biol. Chem. **277**, 8130-8139
43 Cornell, R. B. and Taneva, S. G. (2006) Amphipathic helices as mediators of the membrane interaction of amphitropic proteins, and as modulators of bilayer physical properties. Curr. Protein Pept. Sci. **7**, 539-552
44 Maget-Dana, R. (1999) The monolayer technique: a potent tool for studying the interfacial properties of antimicrobial and membrane-lytic peptides and their interactions with lipid membranes. Biochim. Biophys. Acta **1462**, 109-140
45 Boisselier, É., Demers, É., Cantin, L. and Salesse, C. (2017) How to gather useful and valuable information from protein binding measurements using Langmuir lipid monolayers. Adv. Colloid Interface Sci. **243**, 60-76
46 Silvius, J. R. (1982) Thermotropic Phase Transitions of Pure Lipids in Model Membranes and Their Modifications by Membrane Proteins. John Wiley & Sons, Inc, New York
47 Allen, T., Hwang, H., Jardim, A., Olafson, R. and Ullman, B. (1995) Cloning and expression of the hypoxanthine-guanine phosphoribosyltransferase from *Leishmania donovani*. Mol.

Biochem. Parasitol. **73**, 133-143
48 Hojjat, H. and Jardim, A. (2015) The Leishmania donovani peroxin 14 binding domain accommodates a high degeneracy in the pentapeptide motifs present on peroxin 5. Biochim. Biophys. Acta **1850**, 2203-2212
49 Hojjat, H. and Jardim, A. (2015) Identification of *Leishmania donovani* peroxin 14 residues required for binding the peroxin 5 receptor proteins. Biochem J. **465**, 247-257
50 Gouveia, A. M., Guimaraes, C. P., Oliveira, M. r. E., Sa-Miranda, C. and Azevedo, J. E. (2003) Insertion of Pex5p into the Peroxisomal Membrane Is Cargo Protein-dependent. J. Biol. Chem. **278**, 4389-4392
51 Girzalsky, W., Rehling, P., Stein, K., Kipper, J., Blank, L., Kunau, W.-H. and Erdmann, R. (1999) Involvement of Pex13p in Pex14p Localization and Peroxisomal Targeting Signal 2-dependent Protein Import into Peroxisomes. J. Cell Biol. **144**, 1151-1162
52 Azevedo, J. E. and Schliebs, W. (2006) Pex14p, more than just a docking protein. Biochim. Biophys. Acta. **1763**, 1574-1584
53 Itoh, R. and Fujiki, Y. (2006) Functional Domains and Dynamic Assembly of the Peroxin Pex14p, the Entry Site of Matrix Proteins. J. Biol. Chem. **281**, 10196-10205
54 Jardim, A., Rager, N., Liu, W. and Ullman, B. (2002) Peroxisomal targeting protein 14 (PEX14) from *Leishmania donovani*: Molecular, biochemical, and immunocytochemical characterization. Mol. Biochem. Parasitol. **124**, 51-62
55 Ding, W., Palaiokostas, M., Wang, W. and Orsi, M. (2015) Effects of lipid composition on bilayer membranes quantified by all-atom molecular dynamics. J. Phys. Chem. B. **119**, 15263-15274
56 Beach, D. H., Holz, G. G., Jr. and Anekwe, G. E. (1979) Lipids of *Leishmania* promastigotes. J. Parasitol. **65**, 203-216
57 Kusters, R., Breukink, E., Gallusser, A., Kuhn, A. and de Kruijff, B. (1994) A dual role for phosphatidylglycerol in protein translocation across the Escherichia coli inner membrane. J. Biol. Chem. **269**, 1560-1563
58 Rietveld, A. G., Koorengevel, M. C. and de Kruijff, B. (1995) Non-bilayer lipids are required for efficient protein transport across the plasma membrane of *Escherichia coli*. EMBO J. **14**, 5506-5513
59 Erdmann, R. and Schliebs, W. (2005) Peroxisomal matrix protein import: the transient pore model. Nat. Rev. Mol. Cell. Biol. **6**, 738-742
60 de Duve, C. and Baudhuin, P. (1966) Peroxisomes (microbodies and related particles). Physiol. Rev. **46** 323-357
61 Hardeman, D., Versantvoort, C., van den Brink, J. M. and van den Bosch, H. (1990) Studies on peroxisomal membranes. Biochim. Biophys. Acta. **1027**, 149-154
62 Zinser, E., Sperka-Gottlieb, C. D., Fasch, E. V., Kohlwein, S. D., Paltauf, F. and Daum. (1991) Phospholipid synthesis and lipid composition of subcellular membranes in the unicellular eukaryote *Saccharomyces cerevisiae*. J. Bacteriol. **173**, 2026-2034
63 Mast, F. D., Fagarasanu, A. and Rachubinski, R. (2010) The peroxisomal protein importomer: a bunch of transients with expanding waistlines. Nat. Cell Biol. **12**, 203-205
64 Meinecke, M., Bartsch, P. and Wagner, R. (2016) Peroxisomal protein import pores. Biochim. Biophys. Acta **1863**, 821-827
65 Francisco, T., Rodrigues, T. A., Dias, A. F., Barros-Barbosa, A., Bicho, D. and Azevedo, J. E. (2017) Protein transport into peroxisomes: Knowns and unknowns. BioEssays. **39**, 1700047
66 Opperdoes, F. R., Baudhuin, P., Coppens, I., De Roe, C., Edwards, S. W., Weijers, P. J. and

Misset, O. (1984) Purification, morphometric analysis, and characterization of the glycosomes (microbodies) of the protozoan hemoflagellate *Trypanosoma brucei*. J. Cell Biol. **98**, 1178-1184

Table I. Phospholipid composition glycosomal/peroxisomal membranes

Phospholipid	PC	PE	PG	PS	PI	PA	CL	Reference
R. norvegicus	61	30	-	3	5	-	-	[61]
S. cerevisiae	48	23	-	4	16	2	7	[62]
T. brucei	61	13	-	7	19	-	-	[66]
L. donovani	52	25	15	-	8*	-	-	This study

* This includes IPC.

Table II Fatty acid composition of the *L. donovani* glycosomal membrane

Fatty acid	% of total
C14:0	2.8 ± 0.1
C16:0	7.1 ± 0.7
C17	0.8 ± 0.2
C18:0	12.8± 0.3
C18:1	25.5± 1.3
C18:2	17.9 ± 0.4
C18:3	6.9 ± 0.1
C19- cyclopropyl	2.8 ± 0.5
C20:2	0.9 ± 0.1
C20:4	0.7 ± 0.2
C22:2	1.2 ± 0.3
C22:4	4.5 ± 0.2
C22:5	14.5 ± 0.3
C22:6	1.7 ± 0.2
C24:0	2.1 ± 0.7

Analysis was performed in triplicate.

Figure legends

Fig. 1. Purification of *L. donovani* glycosomes.
(A) Isolation of glycosomes from *L. donovani* promastigotes was performed by layering the 45,000 x *g* organelle pellet onto a 25-70% (w/v) sucrose gradient and resolving organelles by centrifugation, fractionated from the top and the protein concentration and acid phosphatase activity determined. (B) Aliquots of the whole cell lysate (lysate), 5,000 x *g* nuclear pellet (nuclei), 45,000 x *g* supernatant (45k *g*S) and 45,000 x *g* pellet (45k *g*P) and sucrose gradient fractions were resolved by SDS-PAGE and Western blot performed using anti-LdPEX14 (glycosome), anti-COX IV (mitochondria), anti-Bip (endoplasmic reticulum), and anti-tubulin (plasma membrane or flagella). (C) Enrichment of glycosomes isolated from the Optiprep gradient was assessed using 5 μg of purified glycosomes (glycosomes), 45,000 *x g* organelle pellet (45k *g*P), and whole cell lysate (lysate) and blots were sequentially probed with anti-LdPEX14 and anti-aldolase, and anti-tubulin.

Fig. 2. Lipidomic analysis of *L. donovani* glycosomal membrane.
(A) Phospholipids extracted from purified glycosomes were resolved by 2D-TLC on Silica G thin layer chromatography plates and spots were visualized by charring with sulfuric acid. Analysis of the phospholipid classes and fatty acid modifications were determined by electrospray ionization mass spectroscopy (ESI-MS/MS) and survey scans were obtained in (B) negative ion mode to characterize phosphatidylethanolamine (PE), phosphatidylglycerol (PG), phosphatylinositol (PI) and inositol-phosphoceramide (IPC) lipids and (C) positive ion mode to identify phosphatidylcholine (PC) lipids.

Fig. 3. Interaction of LdPEX14 with large unilamellar vesicles (LUVs).
(A) LdPEX14 binding to LUVs was assessed at 20 °C in the absence (NL) or the presence of 150 or 500 mM NaCl prior to flotation on a sucrose density gradient. (B) The effect of temperature on membrane binding was assessed by pre-incubating LdPEX14 with LUVs at 0, 23 or 37 °C for 40 min prior to density flotation centrifugation and Western blot analysis. (C) The interaction of LdPEX14 with the lipid bilayers was examined by sequential extraction of LdPEX14 loaded LUVs with 500 mM NaCl, 100 mM alkaline carbonate and 100 mM alkaline carbonate / 4.0 M urea. Extracts were separated into supernatant (S) and pellet (P) by centrifugation at 100,000 x *g* prior to Western blot analysis with anti-LdPEX14 antibodies. (D) The association of LdPEX14 with the lipid bilayer was examined using the protease clostripain treatment in the absence (NL) or presence (L) of LUVs. Band intensities were quantified using the ImageJ software.

Fig. 4. Analysis of the LdPEX14 hydrophobic domain.
(A) Secondary structure and transmembrane topology predictions of ldpex14 (120-200) were performed using the Jufo9D, I-TASSER 5.1, TMHHM 2.0 and TOPCONS2 programs. *E* denotes extended strands, *H* alpha-helix and *C* random coils; *o* denotes outside face the membrane, *M* transmembrane and *i* inside face of the membrane (B) Hydrophobicity analysis was predicted by the Kyte and Doolittle (solid line) algorithm [38]. (C) I-TASSER *in silico* model of the LdPEX14 residues 154-174 is predicted to adopt a helical structure with a helix length of 22.4 Å, sufficient to span a lipid bilayer. Molecular graphics were performed using the PyMOL software (v1.8.6).

Fig. 5. The hydrophobic domain and anionic phospholipids are required for membrane binding.

(A) LdPEX14, ldpex14 (Δ149-179), or ldpex14 (120-200) were incubated with and without DOPE:DOPC:DOPG:PI:Chl (55:25:15:2.5:2.5) LUVs, resolved by sucrose density flotation and the distribution of LdPEX14 and ldpex14 (Δ149-179) assessed by Western blot analysis using anti-LdPEX14 or anti-His_6 (ldpex14 120-200). (B) LdPEX14 was incubated with LUVs prepared with the single phospholipids DOPC, DOPE, DOPA, DOPG or DOPS or (C) a mixture of DOPE:DOPC, DOPC:DOPG, or DOPE:DOPG for 40 min at 20 °C then resolved by sucrose density centrifugation.

Figure 6: Fluorescence Activated Cell Sorting (FACS) analysis of LdPEX5 and LdPEX14 with LUVs. DOPE:DOPC:DOPG:PI:cholesterol (55:25:15:2.5:2.5) 200 nm LUVs (400 μg) prepared by extrusion were incubated in PBS (A) or with Oregon Green tagged LdPEX5 (5 μg) (B), Bodipy 630/650 tagged LdPEX14 (5 μg) (C), or a mixture of fluorescently tagged LdPEX5 (5 μg)/LdPEX14 (5 μg) (D), and the bound proteins were analyzed on a BD FACSAria instrument. Gates were established as described in the Experimental procedures section and the percent distribution of the LUV populations are given in the top right hand corner of each panel.

Fig. 7. Interaction of LdPEX14 with lipid monolayers.
(A) Determination of $\Delta\Pi_0$, maximum insertion pressure (MIP) and synergy on a monolayer of DOPG for LdPEX14. (B) Determination of the superficial pressure and the saturating concentration of the air-buffer interface for LdPEX14 (circles) and ldpex14(Δ149-179) (squares) in the absence of phospholipids. (C) Representative raw plots of the evolution of the superficial pressure (Π) over time, upon addition of lipids (DOPG in this case) and protein (final protein concentration : 150 nM for LdPEX14 (black line), 250 nM for ldpex14Δ149-179 (red line)). Dotted lines were added manually to illustrate the rate of penetration of the protein into the phospholipid monolayer.

Fig. 8.
Binding parameters of LdPEX14 to monolayers of different phospholipids.
(A) Maximum insertion pressure and (B) synergy of binding of LdPEX14 to monolayers of different phospholipids. (C) Maximum insertion pressure, (D) synergy of attachment of LdPEX14 to monolayers of PG phospholipids containing different fatty acid chains.

Fig. 9. LdPEX14 promotes membrane binding of LdPEX5 and LdHGPRT.
LUVs were incubated with (A) LdPEX5 or LdHGPRT (PTS1) individually, (B) LdPEX5-LdHGPRT complex, (C) a mixture of LdPEX14 and LdHGPRT, (D) a mixture of LdPEX14 and LdPEX5, (E) mixture of LdPEX14 and an LdPEX5-LdHGPRT complex or (F) with a mixture of ldpex14 Δ149-179 and LdPEX5. Reaction mixtures were resolved by sucrose density flotation centrifugation and the distribution of proteins in the gradients assessed by Western blot analysis anti-LdPEX14 (1:10,000), anti-LdPEX5 (1:10,000) and anti-LdHGPRT (1:2,000) specific antisera.

Figure 10. Membrane insertion of LdPEX5 in LdPEX14 loaded LUVs.
(A) The LdPEX5 motif required for the binding of LUV bound LdPEX14 was localized by mixing ldpex5 variant encompassing residues 205-625 (ldpex5 (205-625)), 268-625 (ldpex5 (268-625)), 303-625 (ldpex5 (303-625)), or 203-391 (ldpex5 (203-391) with LUVs in the presents or absence of LdEX14. (B) LdPEX14 and LdPEX5 were purified by sucrose density flotation. LUVs were

sequentially extracted with 500 mM NaCl, alkaline carbonate pH 11.5, and alkaline carbonate containing 4.0 M urea for 30 min at 0 °C. Following each treatment, samples were separated into supernatant (S) and membrane pellet (P) fractions by centrifugation at 100,000 x g for 30 min at 4 °C and the protein distribution examined by Western blots.

Figure1:

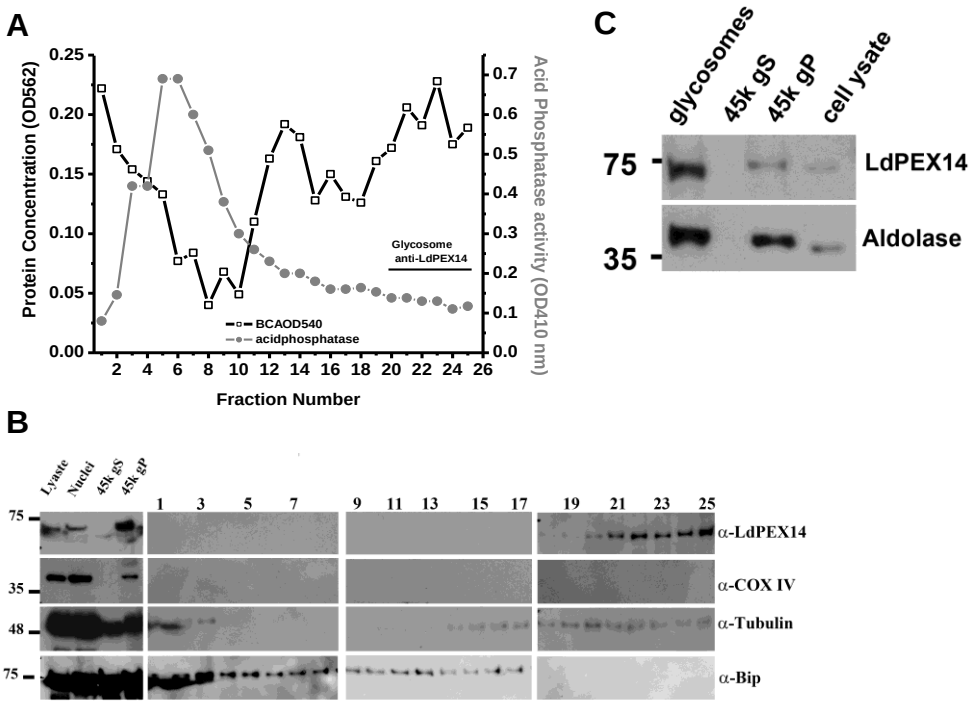

Figure 2

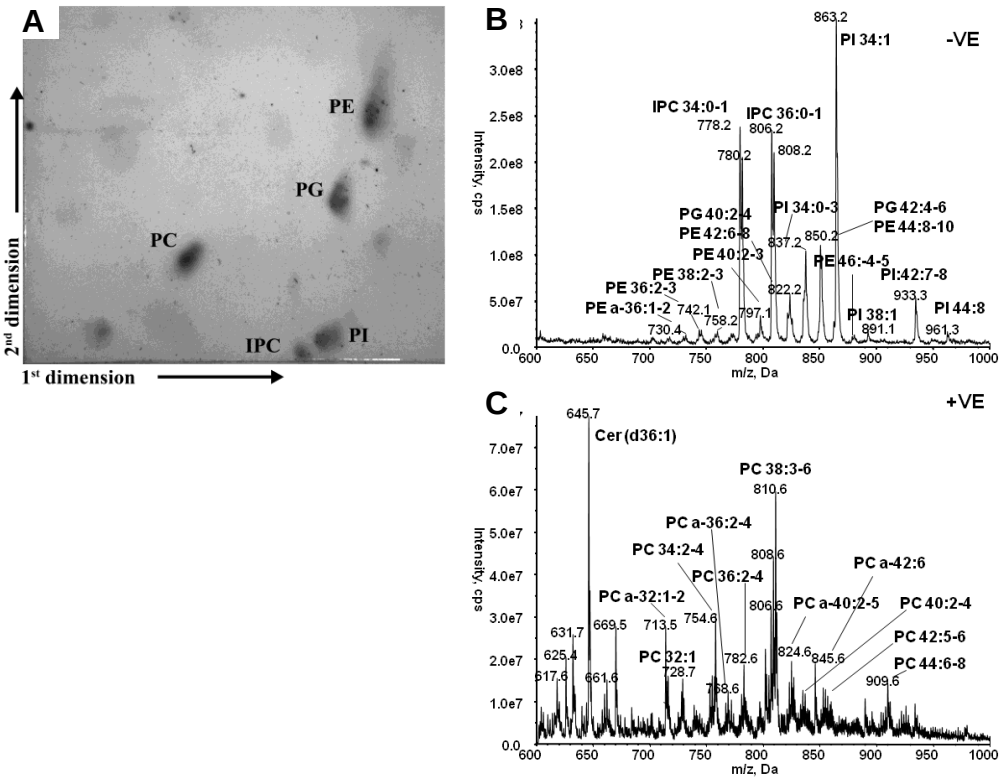

Figure 3

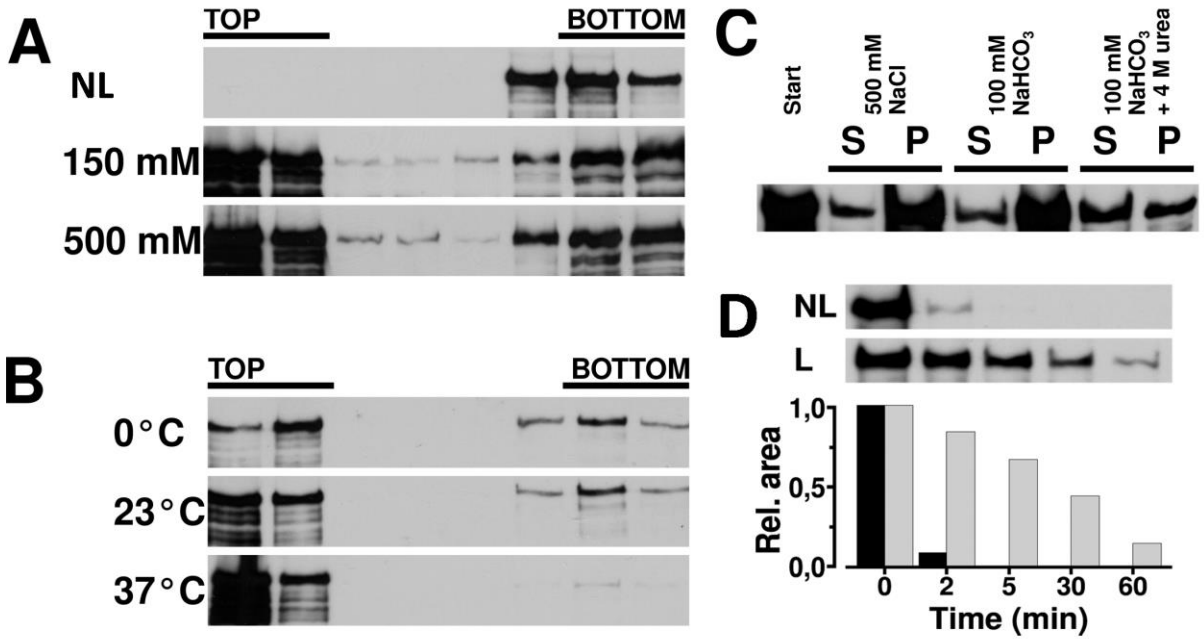

Figure 4:

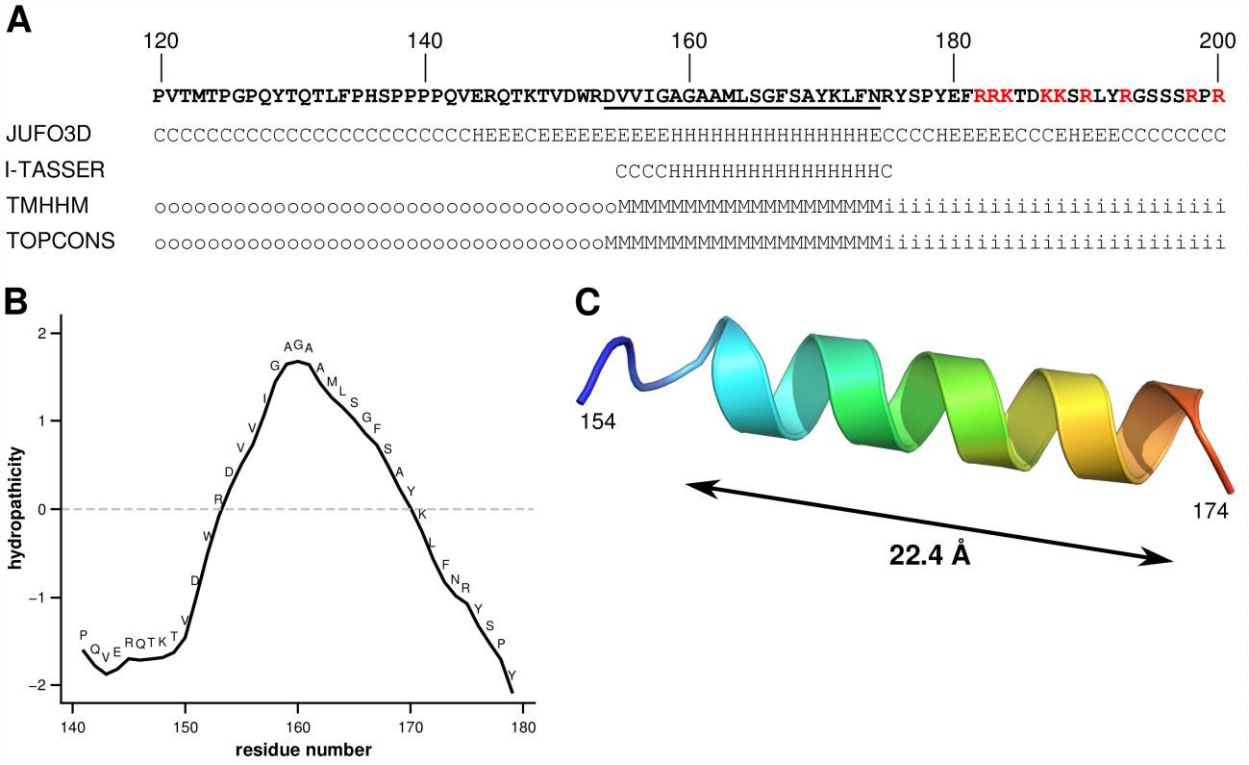

Figure 5:

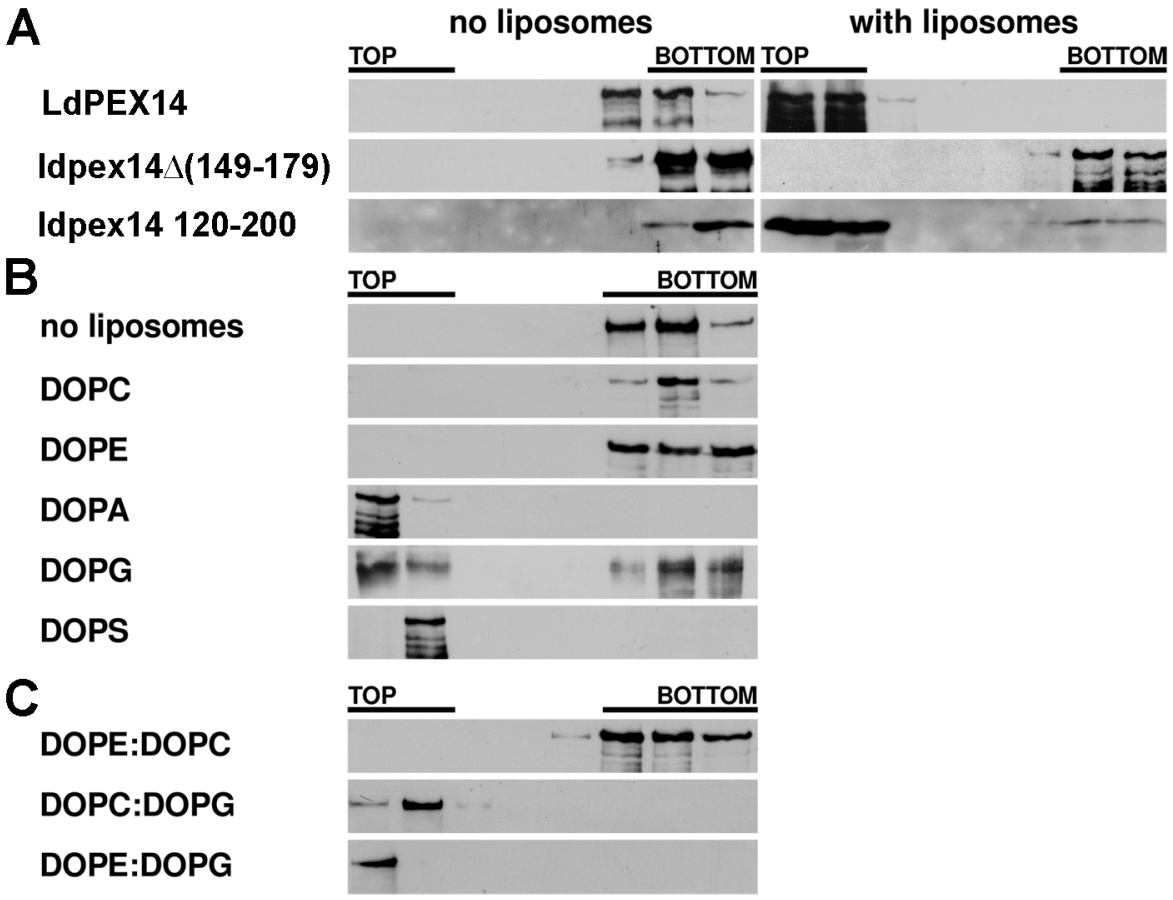
A
no liposomes
with liposomes
TOP
BOTTOM
TOP
BOTTOM
LdPEX14
ldpex14Δ(149-179)
ldpex14 120-200
B
TOP
BOTTOM
no liposomes
DOPC
DOPE
DOPA
DOPG
DOPS
C
TOP
BOTTOM
DOPE:DOPC
DOPC:DOPG
DOPE:DOPG

Figure 6:

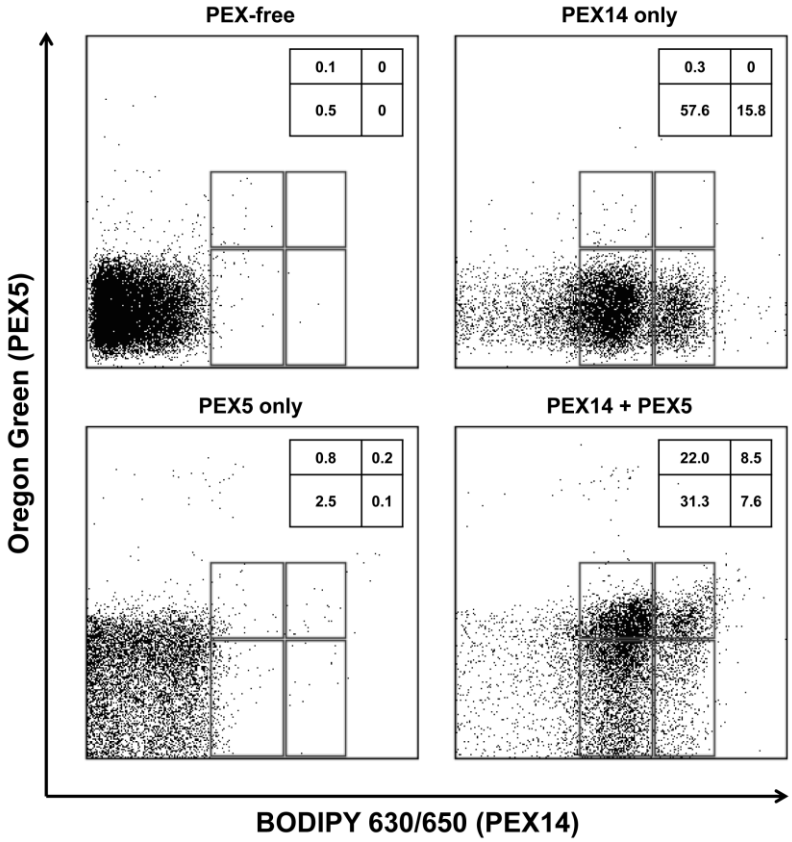
PEX-free
0.1
0
0.5
0
PEX14 only
0.3
0
57.6
15.8
PEX5 only
0.8
0.2
2.5
0.1
PEX14 + PEX5
22.0
8.5
31.3
7.6
Oregon Green (PEX5)
BODIPY 630/650 (PEX14)

Figure 7:

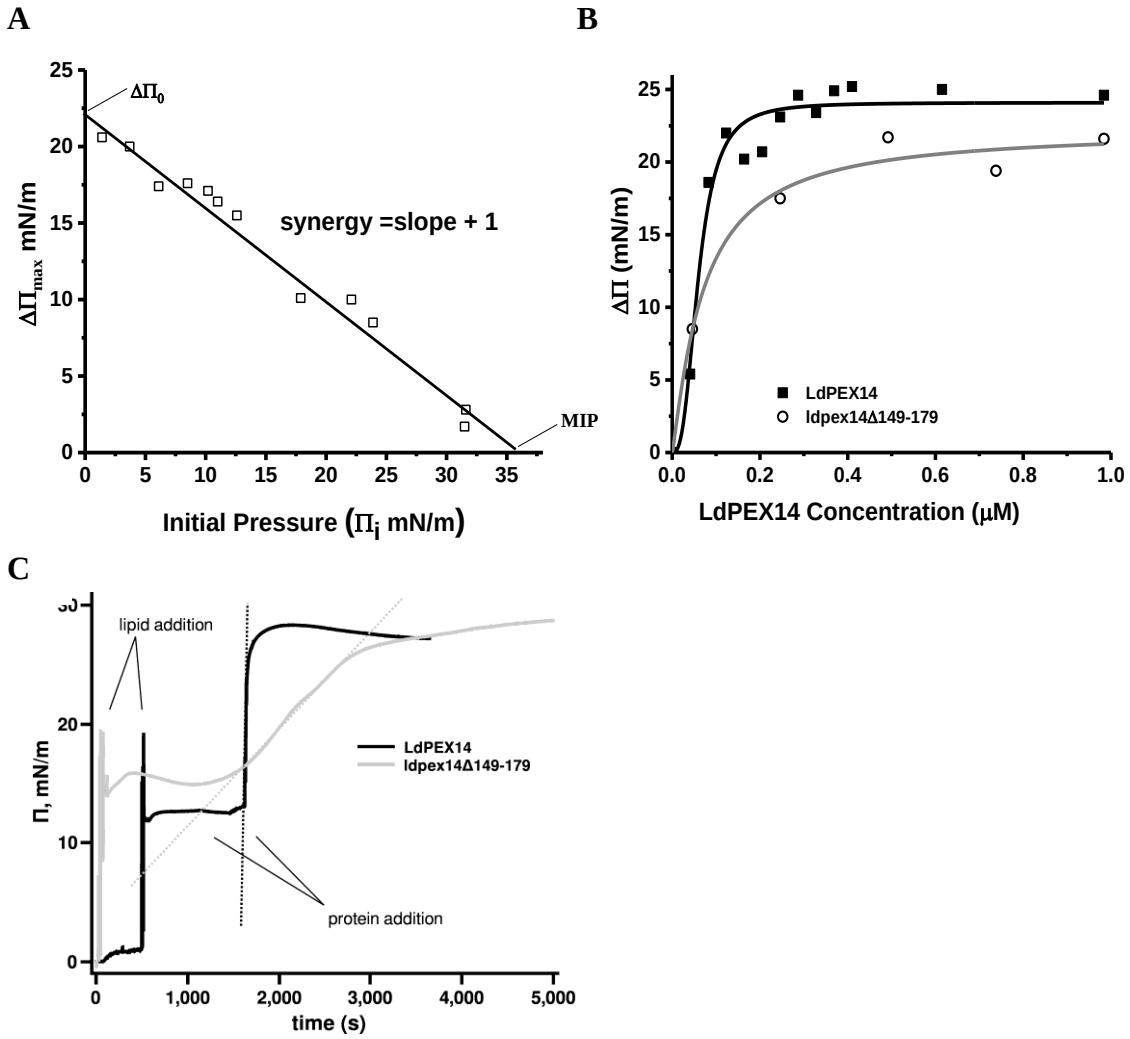
A
ΔΠ0
synergy =slope + 1
MIP
ΔΠmax mN/m
Initial Pressure (Πi mN/m)
B
ΔΠ (mN/m)
LdPEX14
ldpex14Δ149-179
LdPEX14 Concentration (μM)
C
lipid addition
protein addition
LdPEX14
ldpex14Δ149-179
Π, mN/m
time (s)

Figure 8:

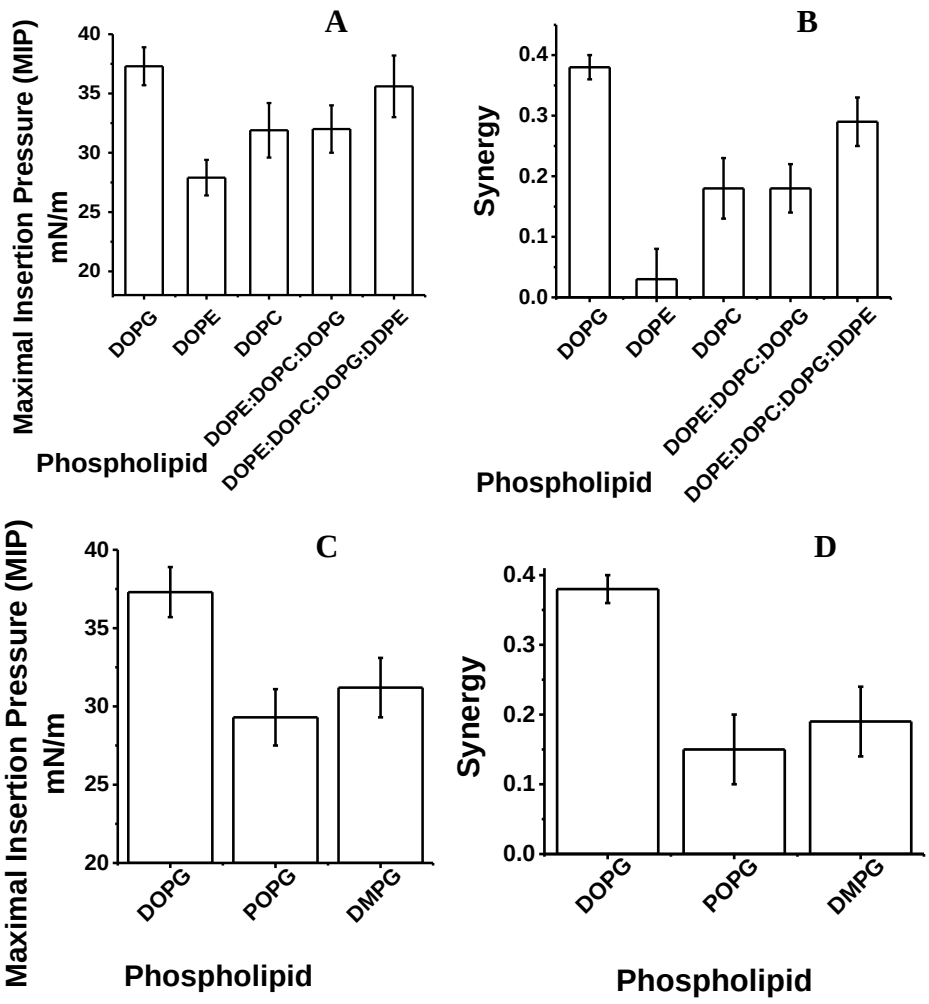
A
B
C
D
Maximal Insertion Pressure (MIP)
mN/m
Synergy
Phospholipid
DOPG
DOPE
DOPC
DOPE:DOPC:DOPG
DOPE:DOPC:DOPG:DDPE
POPG
DMPG

Figure 9:

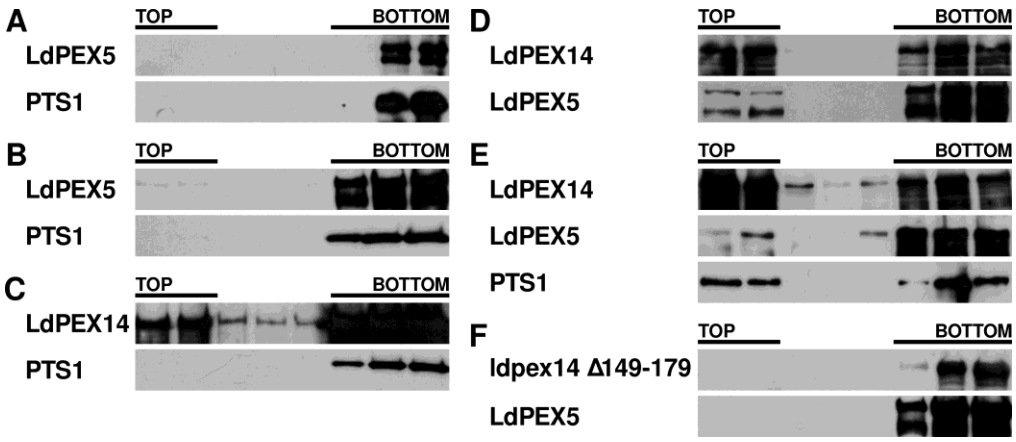

Figure 10: